LA-2414

D-3

LA-2414

Hydrodynamics

LOS ALAMOS SCIENTIFIC LABORATORY
OF THE UNIVERSITY OF CALIFORNIA o LOS ALAMOS NEW MEXICO

THE BOUNDING OF INSTABILITIES OF THE PIC DIFFERENCE EQUATIONS

E-0

LEGAL NOTICE

This report was prepared as an account of Government sponsored work. Neither the United States, nor the Commission, nor any person acting on behalf of the Commission:

A. Makes any warranty or representation, expressed or implied, with respect to the accuracy, completeness, or usefulness of the information contained in this report, or that the use of any information, apparatus, method, or process disclosed in this report may not infringe privately owned rights; or

B. Assumes any liabilities with respect to the use of, or for damages resulting from the use of any information, apparatus, method, or process disclosed in this report.

As used in the above, "person acting on behalf of the Commission" includes any employee or contractor of the Commission, or employee of such contractor, to the extent that such employee or contractor of the Commission, or employee of such contractor prepares, disseminates, or provides access to, any information pursuant to his employment or contract with the Commission, or his employment with such contractor.

~~Printed in USA. Price $1.50.~~ Available from the

Office of Technical Services
U. S. Department of Commerce
Washington 25, D. C.

LA-2414
UC-32, MATHEMATICS AND
COMPUTERS
TID-4500 (19th Ed.)

LOS ALAMOS SCIENTIFIC LABORATORY
OF THE UNIVERSITY OF CALIFORNIA LOS ALAMOS NEW MEXICO

REPORT WRITTEN: December 1962

REPORT DISTRIBUTED: March 27, 1963

THE BOUNDING OF INSTABILITIES OF THE PIC DIFFERENCE EQUATIONS

by

Bart J. Daly

Contract W-7405-ENG. 36 with the U. S. Atomic Energy Commission

ABSTRACT

A study is made of the effect of a nonlinearity on the stability properties of a simplified version of the PIC difference equations. An equilibrium amplitude of the fluctuations, resulting from the instability, is determined as a function of the parameters of the method.

ACKNOWLEDGMENTS

The author wishes to express sincere appreciation for the encouragement and invaluable guidance extended by Francis H. Harlow throughout the preparation of this paper. Grateful acknowledgment is also due to Emma Lou Young for her assistance in assembling data for this report.

CONTENTS

INTRODUCTION

The Particle-in-Cell (PIC) technique is a finite difference method of expressing the equations of motion of a compressible fluid; it has been described in various reports [1,2]. The computational framework for the method is achieved by dividing the system into an Eulerian mesh of cells and superimposing a mesh of particles whose distribution and mass are such as to describe the initial configuration of the fluid. The differential equations of motion, with transport terms neglected, are written in finite difference form relative to the system of cells. The transport effect is obtained by allowing the particles to move through the fixed cellular coordinate system according to the velocities in the neighboring cells.

The method has achieved considerable success in problems involving high velocity fluid flow and it has been recognized [1] that a large portion of this success is attributable to the transport mechanism of the method. The movement of particles across cell boundaries gives rise to a nonlinear dissipative force which is effective in reducing the fluctuations that arise as a result of the differencing technique. This dissipative term is of the form of a "true" viscosity, in that it is proportional to the velocity gradient.

The same measure of success has not been obtained, however, in representing low velocity flow. The primary reason for this is that the velocity gradients are too small to make the dissipative force effective, so that instabilities develop. This difficulty can be overcome by introducing into the equations linear forms of artificial viscosity, whose effect persists even to zero speeds. However, this solution is not always desirable in other regions of the fluid, since the artificial viscosity tends to obliterate some of the features of interest of the high velocity flow.

But the effect of this instability can be minimized, without recourse to artificial viscosity, by the optimum choice of the adjustable parameters of the method. The reason is that the dissipative term prevents unbounded growth of the instability. Hence, if one can determine the upper limit of the fluctuations, which result from this instability, as a function of the parameters of the system, the parameters can then be chosen in such a way as to bound the instability to a tolerable level. The primary purpose of this report is to determine the mechanics of this dissipative process in a finite difference system and thereby achieve an expression for the equilibrium amplitude of fluctuations in terms of the parameters.

This study was further prompted by a desire to learn more about the effect of nonlinearities on difference equation stability in general. This consideration, together with the difficulty involved in the study of more than one nonlinearity at a time, has led us to investigate a

simplified version of the PIC equations rather than the full equations. It is hoped that the results of this analysis will thereby be applicable to a wider range of difference methods.

The appendices to this report deal with certain improvements on the PIC method which have not previously been published. Appendix I is concerned with the form of the energy equation as it appears in this report. This form differs from that which was employed in previous discussions of the PIC method in that it is derived from the differential equation of motion for specific internal energy rather than that for total energy.

Appendix II describes the form and effectiveness of the various types of artificial viscosity which have been employed in PIC calculations at Los Alamos. It also contains a discussion of a more effective manner of expressing the viscosity terms in the difference equations than had been in use previously. This latter section should also be applicable to finite difference methods other than PIC.

PART I. STABILITY ANALYSIS OF THE PIC EQUATIONS

A PIC calculation is performed in three phases. In Phase I the difference form of the momentum and energy equations, exclusive of the transport terms, is solved. Phase II is then concerned with the movement of particles; Phase III deals with the re-partitioning, among the cells, of momentum and energy carried by particles which cross cell boundaries.

The stability properties of the method are completely determined, however, by the first of these phases, since they are concerned with the response of the system to a perturbation of steady state conditions. For, if the fluctuations which result from this perturbation attain sufficient magnitude to cause appreciable movement of particles, then instability is amply demonstrated. But, by restricting the study to the equations of Phase I, the determination of stability becomes a matter of ascertaining whether or not there is growth with time of the magnitude of the fluctuations produced by the perturbation.

Assuming, therefore, that the system will retain its initial uniform density configuration, the one dimensional PIC difference equations can be written,

$$\frac{u^{n+1}_{j-1/2} - u^{n}_{j-1/2}}{\delta t} = \frac{1}{\rho \delta x}\left[\left(p^{n}_{j-1} - p^{n}_{j}\right) + \left(q^{n}_{j-1} - q^{n}_{j}\right)\right],$$

$$\frac{I^{n+1}_{j-1/2} - I^{n}_{j-1/2}}{\delta t} = \frac{1}{\rho \delta x}\left[p^{n}_{j-1/2}(\bar{u}_{j-1} - \bar{u}_{j}) + q^{n}_{j-1}\bar{u}_{j-1}\right. \qquad (1)$$

$$\left. - q^{n}_{j}\bar{u}_{j} + \bar{u}_{j-1/2}\left(q^{n}_{j} - q^{n}_{j-1}\right)\right],$$

where $u^{n}_{j-1/2}$, $I^{n}_{j-1/2}$ and $p^{n}_{j-1/2}$ represent the velocity, specific internal energy, and pressure at the center of the jth cell at time $t = n\delta t$. Also,

$$\bar{u}_{j-1/2} = \frac{1}{2}\left(u^{n+1}_{j-1/2} + u^{n}_{j-1/2}\right),$$

$$q^{n}_{j} = \rho\left(ac_{0} + \frac{f}{2}\left|u^{n}_{j-1/2} + u^{n}_{j+1/2}\right|\right)\left(u^{n}_{j-1/2} - u^{n}_{j+1/2}\right),$$

where a and f are constants of approximately unit magnitude and c_0 is a fixed representative sound speed for the system.

The q terms represent artificial viscosity; their purpose is to improve the stability and accuracy of the method by smoothing out any fluctuations which may develop in the system. A discussion of the form of these terms and the manner in which they are expressed in the difference equations will be found in Appendix II, but it is pertinent to this section to point out one particular aspect of their expression which complicates the analysis. Artificial viscosity is usually applied only in those parts of the system that are undergoing compression; in those regions which are experiencing rarefaction, additional dissipation is not required.

The dilemma which arises in a stability analysis is that there is no clearcut way of expressing, in the equations, the fact that the q terms are nonzero only when their velocity gradient factor is positive. The course which is sometimes followed in such a situation is to assume that, in a perturbed stagnation, each point in the system experiences equal periods of compression and rarefaction. Then, for the purpose of the analysis, the dissipative mechanism is applied at all times but only one-half the actual coefficient of viscosity is used. For lack of an alternative, this procedure will be followed in the present analysis, but the amount of error thereby introduced will be demonstrated by experiment.

To proceed with the stability analysis, let us consider a system, described by Eqs. (1), which has been perturbed from steady state. The perturbation is introduced by means of the substitution

$$u^n_{j-1/2} \rightarrow u_0 + \delta u^n_{j-1/2},$$

$$I^n_{j-1/2} \rightarrow I_0 + \delta I^n_{j-1/2},$$

where u_0 and I_0 are the steady state values and

$$\frac{\delta u^n_{j-1/2}}{\sqrt{I_0}}, \frac{\delta I^n_{j-1/2}}{I_0} \ll 1.$$

Then, retaining only first order terms in the variation of these small values, Eqs. (1), with a polytropic equation of state, $p = (\gamma - 1)\rho I$, become

$$\delta u_{j-1/2}^{n+1} = \delta u_{j-1/2}^{n} + \sigma\left(\delta I_{j-3/2}^{n} - \delta I_{j+1/2}^{n}\right) + \lambda\left(\delta u_{j-3/2}^{n} + \delta u_{j+1/2}^{n} - 2\delta u_{j-1/2}^{n}\right),$$

$$\delta I_{j-1/2}^{n+1} = \delta I_{j-1/2}^{n} + \frac{\sigma I_0}{2}\left(\delta u_{j-3/2}^{n+1} + \delta u_{j-3/2}^{n} - \delta u_{j+1/2}^{n+1} - \delta u_{j+1/2}^{n}\right), \tag{2}$$

where $\sigma = \dfrac{(\gamma - 1)\delta t}{2\delta x}$,

$$\lambda = \frac{1}{2}\left(ac_0 + f\left|u_0\right|\right)\frac{\delta t}{\delta x}.$$

Assuming that a solution of Eqs. (2) can be expressed in terms of Fourier series, let us examine the conditions under which a typical term can be a solution. Take as the representative terms from the series

$$\delta u_{j-1/2}^{n} = A\, e^{ik(j-1/2)}\, r^{n}, \tag{3}$$

$$\delta I_{j-1/2}^{n} = B\, e^{ik(j-1/2)}\, r^{n}.$$

Then expressing Eqs. (2) in terms of solution (3), we obtain

$$A(r - 1) = \sigma B(e^{-ik} - e^{ik}) + \lambda A(e^{-ik} + e^{ik} - 2),$$

$$B(r - 1) = \frac{\sigma I_0}{2}\, A\left[(e^{-ik} - e^{ik})\,(r + 1)\right],$$

and, on collecting terms, this becomes

$$\begin{aligned} A[r - 1 + 2\lambda(1 - \cos k)] + B(2i\sigma \sin k) &= 0, \\ A[i\sigma I_0(r + 1) \sin k] \quad + B(r - 1) \quad &= 0. \end{aligned} \tag{4}$$

A necessary and sufficient condition that Eqs. (4) have a nontrivial solution for A and B is that

$$(r - 1)^2 + 2\lambda(1 - \cos k)\,(r - 1) + 2\sigma^2 I_0\,(\sin^2 k)\,(r + 1) = 0\,.$$

From this equation a solution can be obtained for r in the form

$$r = 1 - \alpha - \beta \pm \sqrt{(\alpha + \beta)^2 - 4\beta}, \tag{5}$$

where $\alpha = \lambda(1 - \cos k)$,

$$\beta = \sigma^2 I_0 \sin^2 k.$$

In order that solution (3) does not grow with time it is necessary that $|r| \leq 1$. The restrictions, which this condition imposes upon the parameters, depend on whether r is a real or complex number.

Case I: $(\alpha + \beta)^2 < 4\beta$

Then r is complex and

$$|r|^2 = 1 - 2\alpha + 2\beta$$
$$= 1 - 2\lambda(1 - \cos k) + 2\sigma^2 I_0(1 - \cos^2 k).$$

Thus, in order that $|r|^2 \leq 1$, it is required that

$$\lambda \geq \sigma^2 I_0(1 + \cos k).$$

Now, the boundary conditions on a PIC problem require that the velocity vanish at the ends of the system. This limits the allowable values of k to the values

$$k = \frac{\pi}{N}, \frac{2\pi}{N}, \cdots,$$

where N is the number of cells in the system. Thus, to insure stability for all values of k, it is sufficient to require that the inequality

above holds when $k = \frac{\pi}{N}$.* The stability property for Case I then becomes

$$ac_0 + f|u_0| \geq \left(1 + \cos \frac{\pi}{N}\right) \frac{(\gamma - 1)^2 I_0 \, \delta t}{2\delta x} .$$

But at steady state $u_0 \equiv 0$, so for Case I the stability requirement is

$$ac_0 \geq \left(1 + \cos \frac{\pi}{N}\right) \frac{(\gamma - 1)^2 I_0 \, \delta t}{2\delta x} . \qquad (6)$$

Case II: $(\alpha + \beta)^2 > 4\beta$

In this case r is real and $\partial r/\partial k$ is proportional to sin k, so that $|r|$ attains its maximum value at $k = \pi$. For this value of k the requirement that $|r| < 1$ reduces to the condition

$$0 < 2\lambda < 1,$$

i.e.,

$$0 < ac_0 < \frac{\delta x}{\delta t}.$$

Notice, in Eqs. (3), that $k = \pi$ corresponds to a solution with a wavelength of 2 cells. Hence it is the high frequency components which are most drastically affected by excessive artificial viscosity. The reason is that the viscosity term is proportional to the velocity gradient between adjacent cells, so that excessive correction results in a gradient of opposite direction but increased magnitude. The resultant of these excessive corrections is a high frequency disturbance which grows exponentially.

---

*Fourier components for which $k = 2\pi n$ correspond to velocity profiles which are identically zero; hence growth of these components will not lead to instability.

The result of violating the condition which is derived in Case I, i.e., too little artificial viscosity, is the subject of Part II. Briefly, rapidly growing fluctuations develop here also, until the velocity magnitudes become large enough to allow the $f|u_0|$ term to stabilize the system. This capacity permits PIC calculations to be performed without any artificial viscosity whatsoever, since a term of the $f|u_0|$ type is inherent in the PIC method of moving the particles (Ref. 1, p. 14 ff).

A plot of the predicted region of stability (for fixed values of γ, δx, N and I_0) is shown in Fig. 1. When, in the machine runs, artificial viscosity is applied in both rarefactions and compressions, it is found that the observed limits of stability agree perfectly with this prediction. But the experimentally observed outline of the region of stability for problems in which artificial viscosity is applied in compressions only is shown by the dashed line. The discrepancy between the area thus outlined and the predicted region of stability indicates that our assumption (that in a perturbed stagnation artificial viscosity applied in compressions only is equivalent to one-half the amount applied in both compressions and rarefactions) does not hold for large amounts of artificial viscosity. The reason is that, when compressions are rapidly damped, the system experiences rarefaction considerably more than fifty percent of the time.

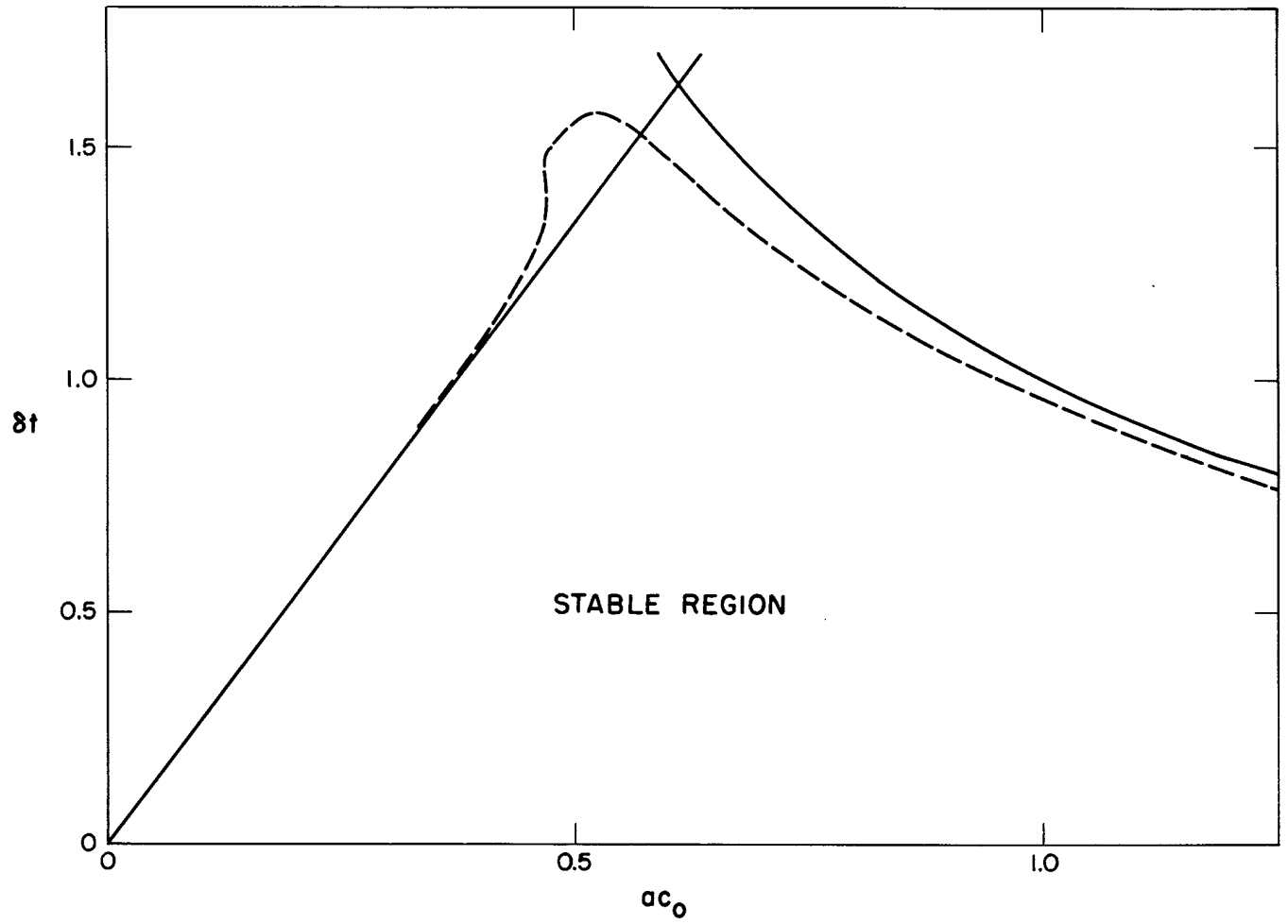

Fig. 1: Plot of the region of stability for $\gamma = 5/3$, $\delta x = 1.0$, $N = 6$, and $I_0 = 0.9$. The solid lines outline the predicted region and the region which is observed when artificial viscosity is applied in both rarefactions and compressions. The dashed line corresponds to the observed limits of stability when artificial viscosity is applied only in compressions.

PART II. THE NONLINEAR BOUNDING OF THE PIC INSTABILITY

The stability analysis of Part I indicated that the PIC equations were unstable when the coefficient of the linear part of the artificial viscosity term was less than a certain positive definite function of the parameters of the system. It was also observed, however, that this instability was bounded in amplitude by the nonlinear part of the viscosity terms, which corresponds to the effective viscosity of PIC. It is the purpose of this section of the report to study the mechanics of this damping force and to obtain an expression for the equilibrium amplitude of fluctuations in terms of the parameters of the system.

To attempt an analysis of the complete PIC equations, including a provision for density variation, would be a very complicated procedure. Instead, the study will be concerned with the effects of the nonlinearity upon a simplified version of these equations, which has the same stability properties as the complete equations. The results can then be extended qualitatively to the complete equations.

Two simplifications are made — the energy equation is linearized, and cell density is fixed as a constant. The first condition has very little effect upon the outcome of experiments, whereas the second amounts

to a removal of the viscosity which is inherent in the PIC equations, so that the nonlinearity is weaker but acts in the same manner. But these changes permit us to restrict our attention to a single nonlinear term, thereby simplifying the analysis and generalizing the study. As a result the conclusions will be applicable to a wider class of nonlinear problems.

Our purpose is to consider these equations for a fluid which has been perturbed slightly from steady state. The linear part of the artificial viscosity is set to zero (so the system is unstable) but the nonlinear part is present. With the foregoing changes and a polytropic equation of state, Eqs. (1) become

$$\frac{u^{n+1}_{j-1/2} - u^{n}_{j-1/2}}{\delta t} = \frac{\gamma - 1}{2\delta x}\left(I^{n}_{j-3/2} - I^{n}_{j+1/2}\right) + \frac{f}{2\delta x}\left[\left|u^{n}_{j-3/2} + u^{n}_{j-1/2}\right| \times \left(u^{n}_{j-3/2} - u^{n}_{j-1/2}\right) - \left|u^{n}_{j-1/2} + u^{n}_{j+1/2}\right|\left(u^{n}_{j-1/2} - u^{n}_{j+1/2}\right)\right], \tag{7}$$

$$\frac{I^{n+1}_{j-1/2} - I^{n}_{j-1/2}}{\delta t} = \frac{(\gamma - 1)I_0}{2\delta x}\left(\bar{u}_{j-3/2} - \bar{u}_{j+1/2}\right),$$

where I_0 is the initial value of specific internal energy.

Computer Results

A series of problems were run on the computer in order to test the effect of the various parameters on the final equilibrium attained by these equations. An initial perturbation was supplied as a small velocity

in each cell, and the resulting fluctuations were observed through their effect on the kinetic energy histories. In addition, the velocity profiles were analyzed in detail through Fourier decomposition.

Figure 2, curves (a) to (h), shows the kinetic energy histories for a series of machine runs in which the size of the system varies from 6 to 80 cells, all other parameters being fixed at the following values: $\delta t = 0.25$, $\delta x = 1.0$, $f = 1.0$, $\gamma = 1.67$, and $I_0 = 0.9$. Boundary conditions specify $u = 0$ at the ends of the region, and when the linear form of viscosity is included in Eqs. (7) the final equilibrium condition is $u = 0$ everywhere. Thus the kinetic energy $\frac{m}{2} \sum_j u^2_{j-1/2}$, is a good measure of the nonvanishing fluctuation. Since the frequency of oscillations of kinetic energy is too high to plot on the scale of Fig. (2), the curves trace the loci of the maximum and minimum points. The average midpoint between these lines at late times is taken as the equilibrium value.

In these curves, notice that fluctuations grow rapidly at first (as in a linear problem) but are eventually bounded to equilibrium. The amount of overshoot which precedes equilibrium, as well as the mean equilibrium amplitude, generally increase with the size of the system, although the 6 cell system is anomalous in both respects.

The machine results show that the course of any one calculation usually can be divided into three phases. In the first or linear phase, the fluctuations grow rapidly in time. This phase is terminated by the achievement, in the mean, of velocity fluctuations large enough to give appreciable nonlinear dissipation. In the second phase, there is a first

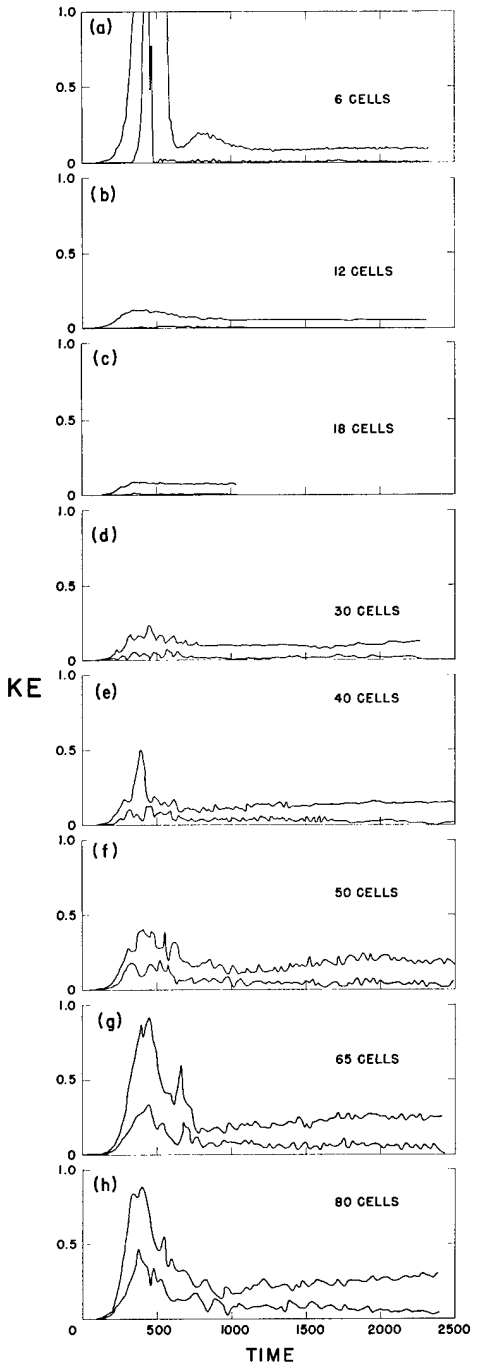

Fig. 2: Kinetic energy histories for PIC-like systems which have been perturbed from steady state. The lines trace the loci of maximum and minimum values of kinetic energy. Input data, other than the number of cells in the system, is the same for all these problems: $\delta x = 1.0$, $\delta t = 0.25$, $\gamma = 5/3$, $ac_0 = 0$, $f = 1.0$, $u_j = 0.01$, $I_j = 0.9$.

order balance between the instability and the dissipation, but also there is a higher order imbalance leading to slow transition to final steady state (the third phase). The origin of these phases will be discussed in more detail in the following sections. Most of the calculations were not run long enough to show the Phase III behavior.

Other experiments were performed in which the time interval and the coefficient of the nonlinear term were varied. It was found that the final equilibrium kinetic energy was proportional to $(\delta t/f)^2$, which behavior is explained within the next few pages.

The initial perturbation in these problems was such that only the symmetric (odd) Fourier modes of oscillation were originally present in the system. Furthermore, the rate of growth of the even modes was observed to be very small compared to that of the odd modes, so that the nonsymmetric modes never contributed significantly to the energy of the system. A Fourier analysis of velocity profiles showed that, among the odd modes at late times, one mode of oscillation usually was dominant. When the number of cells in the system was small, the lowest frequency mode was predominant, exceeding the other modes in amplitude by several orders of magnitude; but in larger systems one of the higher frequency modes generally dominated. In these latter cases the amplitude of the dominant mode was usually two or three times that of the next largest mode. Also, although the wave number of the dominant mode differed from problem to problem, it was found that its late time amplitude was always nearly the same. These features are illustrated in Table 1.

TABLE 1

AMPLITUDE OF SIGNIFICANT MODES AT COMPLETION OF MACHINE RUNS FOR SEVERAL PROBLEMS

The amplitudes shown in parentheses are averages of highly oscillating values.

Mode No.	Number of Cells in System (Duration of Problem in Time Cycles)				
	12 (9200)	30 (9150)	40 (13,700)	65 (9700)	80 (9900)
1	0.140	---	0.015	---	---
3	(0.002)	0.023	0.014	0.006	---
5	0.000	0.073	0.051	0.013	---
7	0.000	0.107	0.121	0.022	---
9	(0.001)	0.024	0.011	0.032	0.007
11	(0.001)	(0.009)	0.001	0.048	0.028
13		(0.002)	0.004	0.108	0.109
15		(0.004)	0.001	0.033	0.032
17		(0.006)	(0.002)	0.015	0.033
19		(0.010)	(0.002)	0.032	0.036
21		(0.011)	(0.003)	(0.003)	(0.009)
23		(0.007)	(0.001)	(0.002)	(0.007)
25		(0.005)	(0.001)	(0.002)	(0.006)
27		(0.003)	(0.002)	(0.002)	---
29		(0.002)	0.000	(0.003)	---

The Mechanics of Dissipation

In the analysis of the problem of equilibrium balance, it will turn out to be sufficiently accurate to consider an approximation to Eqs. (7). We therefore expand Eqs. (7) in Taylor series about the center of the jth cell and about time nδt. Neglecting terms higher than the first in δx and δt, we have

$$\frac{\partial u^n_{j-1/2}}{\delta t} + \frac{\delta t}{2}\frac{\partial^2 u^n_{j-1/2}}{\partial t^2} = -(\gamma - 1)\frac{\partial I^n_{j-1/2}}{\partial x} + f\,\delta x \frac{\partial}{\partial x}\left(\left|u^n_{j-1/2}\right| \frac{\partial u^n_{j-1/2}}{\partial x}\right),$$

$$\frac{\partial I^n_{j-1/2}}{\partial t} = -(\gamma - 1) I_0 \frac{\partial u^n_{j-1/2}}{\partial x}. \tag{8}$$

Now, to zero order

$$\frac{\partial u^n_{j-1/2}}{\partial t} = -(\gamma - 1)\frac{\partial I^n_{j-1/2}}{\partial x},$$

so that

$$\frac{\partial^2 u^n_{j-1/2}}{\partial t^2} = -(\gamma - 1)\frac{\partial}{\partial x}\left(\frac{\partial I^n_{j-1/2}}{\partial t}\right) = (\gamma - 1)^2 I_0 \frac{\partial^2 u^n_{j-1/2}}{\partial x^2}.$$

With this substitution Eqs. (8) become

$$\frac{\partial u^n_{j-1/2}}{\partial t} = -(\gamma - 1)\frac{\partial I^n_{j-1/2}}{\partial x} + \frac{\partial}{\partial x}\left\{\left[f\,\delta x\left|u^n_{j-1/2}\right| - (\gamma - 1)^2 I_0 \frac{\delta t}{2}\right]\frac{\partial u^n_{j-1/2}}{\partial x}\right\},$$

$$\frac{\partial I^n_{j-1/2}}{\partial t} = -(\gamma - 1) I_0 \frac{\partial u^n_{j-1/2}}{\partial x}. \tag{9}$$

The stability of Eqs. (9) depends upon the sign of the quantity

$$\sigma\left(u^n_{j-1/2}\right) = f\,\delta x\left|u^n_{j-1/2}\right| - (\gamma - 1)^2 I_0 \frac{\delta t}{2}.$$

A stability analysis of these equations for a fixed value of σ will verify this. In Eqs. (9) let

$$u^n_{j-1/2} = A\, e^{ikx}\, e^{\omega t},$$

$$I^n_{j-1/2} = B\, e^{ikx}\, e^{\omega t}.$$

Then

$$A[\omega + \sigma k^2] + B[ik(\gamma - 1)] = 0,$$

$$A[ik(\gamma - 1)I_0] + B\omega = 0.$$

For a nontrivial solution we must have

$$\omega(\omega + \sigma k^2) + k^2(\gamma - 1)^2 I_0 = 0,$$

or

$$\omega = -\frac{1}{2}\sigma k^2 \pm \frac{1}{2}\sqrt{\sigma^2 k^4 - 4k^2(\gamma - 1)^2 I_0}\,.$$

Now for stability, the real part of ω must be negative. This will be true only when $\sigma > 0$.

Since at steady state $\sigma\left(u^n_{j-1/2}\right)$ is definitely negative, the system is initially unstable. But, as the velocities grow, σ increases and equilibrium is attained at $\sigma = 0$. The corresponding mean velocity magnitude at equilibrium is therefore given by

$$|u| = \frac{(\gamma - 1)^2 I_0\, \delta t}{2f\, \delta x}. \qquad (10)$$

If we assume a probability distribution P(u) of velocities about this mean, the associated mean kinetic energy for a system of N cells of mass m each is given by

$$\overline{KE} = \frac{1}{2} Nm \int_{-\infty}^{\infty} P(u)\, u^2\, du. \tag{11}$$

For a normal distribution

$$P(u) = 0.538\, \upsilon\, e^{-0.91\, \upsilon^2 u^2},$$

$$\upsilon = \frac{f\, \delta x}{(\gamma - 1)^2 I_0\, \delta t};$$

this gives

$$\overline{KE} = 0.275\, \frac{Nm}{\upsilon^2} = 0.275\, Nm \left[\frac{(\gamma - 1)^2 I_0\, \delta t}{f\, \delta x}\right]. \tag{12}$$

In contrast, for a sharp distribution in which $P(u) = \delta(u - \bar{u})$, we get

$$\overline{KE} = \frac{1}{2} Nm \left[\frac{(\gamma - 1)^2 I_0\, \delta t}{2f\, \delta x}\right]^2 = 0.125\, Nm \left[\frac{(\gamma - 1)^2 I_0\, \delta t}{f\, \delta x}\right]^2. \tag{13}$$

A comparison of these predictions with computer results for typical values of the parameters is shown in Fig. 3. The points in the figure indicate observed values, while the upper line is a plot of relation (12), referring to normal distribution of velocities about the mean, and the lowest line shows the kinetic energy, Eq. (13), which would be attained if all cells had the mean velocity. It is seen that the actual distribution lies between these extremes. The prediction requires further analysis, the results of which are shown by the middle line in the figure and are derived below.

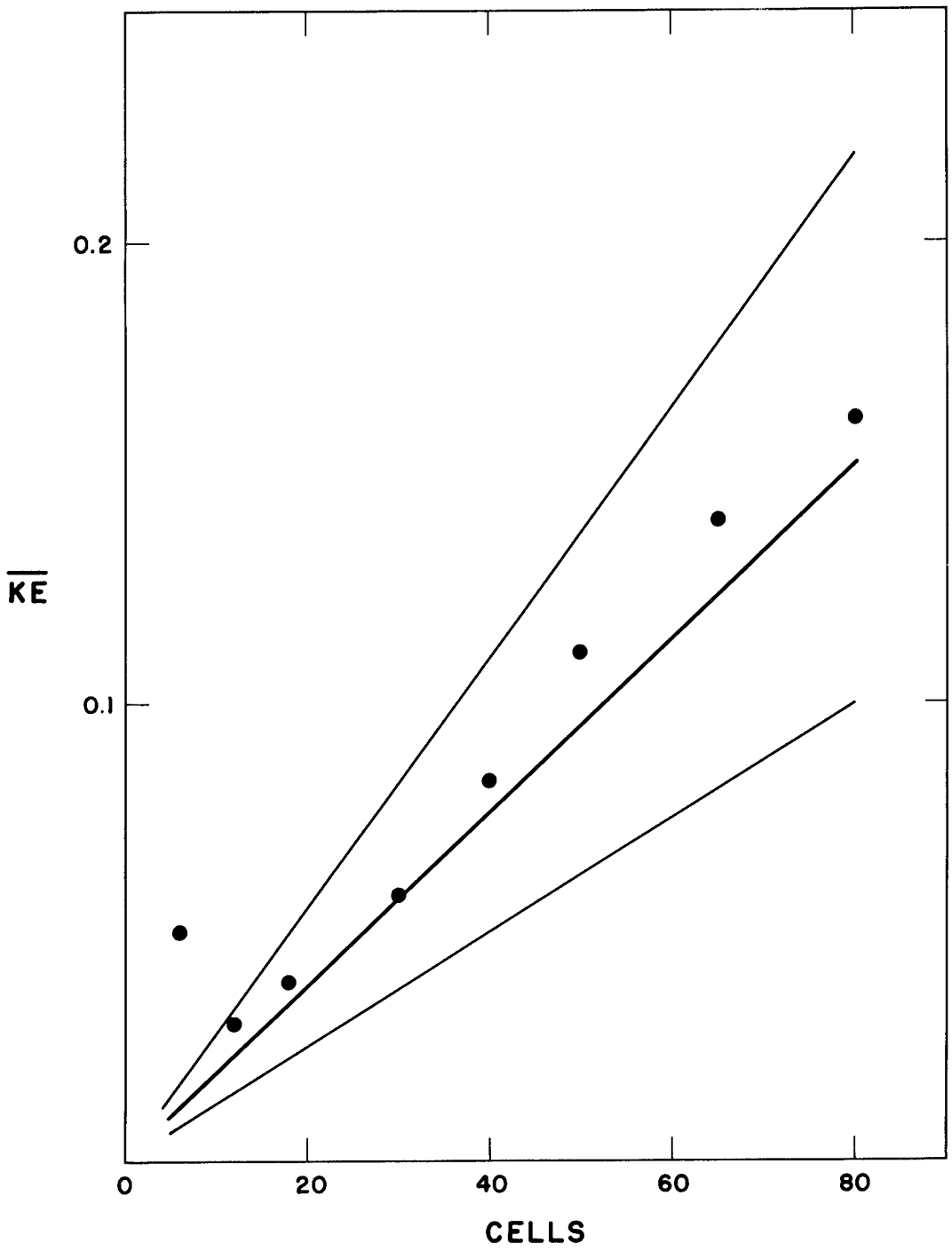

Fig. 3: A comparison of observed values of mean kinetic energy near final equilibrium with three predictions arrived at in the text.

Modal Exchange of Energy

Thus far, the investigation, while shedding some light on the mechanics of the damping process and providing an estimate of the equilibrium amplitude, has told nothing about the normal modes of oscillation in the system or of the energy sharing between these modes. For this purpose we need a more detailed study of the difference equations.

Consider again Eqs. (8),

$$\frac{\partial u}{\partial t} + \frac{\delta t}{2}\frac{\partial^2 u}{\partial t^2} = -(\gamma - 1)\frac{\partial I}{\partial x} + f\,\delta x \frac{\partial}{\partial x}\left(|u|\frac{\partial u}{\partial x}\right), \qquad (8)$$

$$\frac{\partial I}{\partial t} = -(\gamma - 1)I_0 \frac{\partial u}{\partial x}.$$

Notice that we have dropped the subscripts and superscripts for ease of writing.

Following Kryloff and Bogoliuboff [3], we will assume that the solution of these first order equations will not differ much from the solution of the zero order equations, and we will account for this difference by allowing the amplitude and phase of the zero order solution to vary with time. An appropriate solution of the zero order equations is

$$u = A \sin kx \sin(\omega t + \varphi),$$

$$I = \sqrt{I_0}\, A \cos kx \cos(\omega t + \varphi),$$

where

$$\omega = (\gamma - 1)\sqrt{I_0}\, k.$$

The first boundary condition

$$u = 0 \qquad \text{at } x = 0$$

is already satisfied. Applying the boundary condition

$$u = 0 \qquad \text{at } x = L = N\,\delta x$$

determines the unique values which k may assume,

$$k = \frac{n\pi}{L}, \qquad n = 1,2,\cdots .$$

Thus the complete solution of the zero order equations can be written

$$\begin{aligned} u &= \sum_{n=1}^{\infty} A_n \sin\frac{n\pi x}{L} \sin Q_n, \\ I &= \sqrt{I_0} \sum_{n=1}^{\infty} A_n \cos\frac{n\pi x}{L} \cos Q_n, \end{aligned} \tag{14}$$

where

$$Q_n = \frac{n\pi\,(\gamma - 1)\sqrt{I_0}\,t}{L} + \varphi_n = \omega_n t + \varphi_n .$$

Now, considering A_n and φ_n as functions of time, we have

$$\frac{\partial u}{\partial t} = \sum_n \left\{ \sin\left(\frac{n\pi x}{L}\right) \left[\dot{A}_n \sin Q_n + A_n \frac{n\pi(\gamma - 1)\sqrt{I_0}}{L} \cos Q_n + A_n \dot{\varphi}_n \cos Q_n \right] \right\},$$

so that, to impose the zero order solution, it is required that

$$\dot{A}_n \sin Q_n + A_n \dot{\varphi}_n \cos Q_n = 0. \tag{15}$$

Substitution of solution (14), subject to condition (15), into Eqs. (8) gives

$$\sum_n \frac{n\pi(\gamma - 1)\sqrt{I_0}\,\delta t}{2L}\left[\frac{\dot{A}_n}{\cos Q_n} - A_n \frac{n\pi(\gamma - 1)\sqrt{I_0}}{L}\sin Q_n\right]\sin\frac{n\pi x}{L}$$

$$= f\,\delta x \frac{\partial}{\partial x}\left(\left|\sum_n A_n \sin\frac{n\pi x}{L}\sin Q_n\right|\sum_m A_m \frac{m\pi}{L}\cos\frac{m\pi x}{L}\sin Q_m\right)$$

plus an identity equation. Thus

$$\frac{n\pi(\gamma - 1)\sqrt{I_0}\,\delta t}{4}\left[\frac{\dot{A}_n}{\cos Q_n} - A_n \frac{n\pi(\gamma - 1)\sqrt{I_0}}{L}\sin Q_n\right]$$

$$= f\,\delta x \int_0^L \sin\frac{n\pi x}{L}\frac{\partial}{\partial x}\left(\left|\sum_\ell A_\ell \sin\frac{\ell\pi x}{L}\sin Q_\ell\right|\sum_m A_m \frac{m\pi}{L}\cos\frac{m\pi x}{L}\sin Q_m\right)dx.$$

Integration of the right-hand side by parts and simplification give an expression for the rate of growth of the amplitudes,

$$\dot{A}_n = A_n\left(\frac{n\pi(\gamma - 1)\sqrt{I_0}}{2L}\right)\sin 2Q_n - \frac{4f\,\delta x}{L(\gamma - 1)\sqrt{I_0}\,\delta t}\cos Q_n \int_0^L \cos\frac{n\pi x}{L}$$

$$\times\left(\left|\sum_\ell A_\ell \sin\frac{\ell\pi x}{L}\sin Q_\ell\right|\sum_m A_m \frac{m\pi}{L}\cos\frac{m\pi x}{L}\sin Q_m\right)dx. \qquad (16)$$

Consider, first, the case f = 0. Combining Eqs. (15) and (16) we obtain

$$\dot{\varphi}_n = -\omega_n \sin^2(\omega_n t + \varphi_n),$$

which on integration gives

$$\varphi_n = -\omega_n t + \tan^{-1}(\omega_n t + C_n), \qquad (17)$$

where C_n is an arbitrary constant. With this, then

$$\dot{A}_n = \omega_n A_n \left[\frac{\omega_n t + C_n}{1 + (\omega_n t + C_n)^2}\right].$$

Thus

$$A_n = K_n \sqrt{1 + (\omega_n t + C_n)^2}\,, \tag{18}$$

where K_n is a second arbitrary constant.

This shows that with $f = 0$ we can expect a growth in amplitude for each component, becoming linear in time for large times. This solution is also appropriate for $f \neq 0$ when the amplitudes are small enough to neglect the nonlinear term in Eq. (16). But as the amplitudes grow, this nonlinear term will eventually check the instability, bringing the system to equilibrium.

Consider now the case $f \neq 0$. By neglecting cross product terms (whose contribution is small for the significant lower frequency modes), we can write Eq. (16) in a simpler form which illustrates the manner in which fluctuations are damped,

$$\dot{A}_n = A_n \omega_n \sin Q_n \cos Q_n \left[1 - \frac{4f\,\delta x}{L(\gamma - 1)\sqrt{I_0}\,\delta t} \int_0^L |u| \cos^2 \frac{n\pi x}{L}\, dx\right]. \tag{16'}$$

The amplitudes increase in magnitude until the velocity becomes large enough to make the bracket term small. Thus, the mean value of $\dot{A}_n$ approaches zero to first order and A_n achieves its maximum value. The order in which the modes are maximized depends upon the configuration of the velocity profile and of this we can say very little at first. But the velocity magnitude must continue its growth as long as there is a single

mode for which $\dot{A}_n > 0$; during this period the bracket terms become negative for many modes and these oscillations decay.

Herein, perhaps, lies the explanation of the origin of the dominant mode oscillation, which was discussed earlier. For consider the system at the time when there is but a single mode which remains to be maximized. The velocity is increasing in magnitude but all other frequency oscillations are declining, and hence the velocity profile is approaching closer and closer to the configuration of the growing oscillation. It can be shown that the integral in Eq. (16') is least when the velocity is composed entirely of $\frac{2\pi n}{L}$ frequency oscillations; therefore the growing resemblance of the velocity to this frequency only serves to prolong the growth of this final mode and the decay of all other modes. Thus the end of the first phase of the process, which corresponds to the time of maximum velocity magnitude, finds a major portion of the energy of the system concentrated into a single mode; this concentration increases throughout Phase II.

To include the cross product terms and perform the analysis in general would be difficult; however, when a particular mode, say number α, dominates the system to the extent that

$$\left| \sum_{\ell} A_\ell \sin \frac{\ell \pi x}{L} \sin Q_\ell \right| \rightarrow A_\alpha \left| \sin \frac{\alpha \pi x}{L} \sin Q_\alpha \right|, \tag{19}$$

then considerable simplification is possible. Making use of this "dominant-mode" assumption, which will be done for the rest of this paper, Eq. (16) can be written

$$\dot{A}_n = A_n \omega_n \sin Q_n \cos Q_n - \frac{4f\,\delta x}{L(\gamma - 1)\sqrt{I_0}\,\delta t} \cos Q_n A_\alpha \left|\sin Q_\alpha\right| \tag{20}$$

$$\times \sum_m \psi_m \int_0^L \left|\sin \frac{\alpha \pi x}{L}\right| \cos \frac{m\pi x}{L} \cos \frac{n\pi x}{L}\, dx,$$

where

$$\psi_m = \frac{m\pi}{L} A_m \sin Q_m.$$

Now

$$\int_0^L \left|\sin \frac{\alpha \pi x}{L}\right| \cos \frac{m\pi x}{L} \cos \frac{n\pi x}{L}\, dx$$

$$= \frac{1}{\alpha\pi} \sum_{i=1}^{\alpha} \left[\frac{\cos i\left(\frac{m+n}{\alpha}\right)\pi}{1 - \left(\frac{m+n}{\alpha}\right)^2} + \frac{\cos i\left(\frac{m-n}{\alpha}\right)\pi}{1 - \left(\frac{m-n}{\alpha}\right)^2} \right],$$

and

$$\sum_{i=1}^{\alpha} \cos i\left(\frac{m \pm n}{\alpha}\right)\pi = \begin{cases} \alpha, & \text{for } \frac{m \pm n}{\alpha} = k, \text{ an integer,} \\ 0, & \text{otherwise.} \end{cases}$$

In the machine calculations, it was observed that the even modes never contributed significantly to the fluctuation energy. This is reasonable to expect, since the equations with f = 0 conserve symmetry and initially only odd modes were present; by the time even modes could couple in significantly, equilibrium of Phase II type had been achieved and further even-mode growth was slowed to second order. Thus, with only odd modes considered, the sum in Eq. (20) can be written

$$S_n \equiv \sum_m \psi_m \int_0^L \left|\sin \frac{\alpha\pi x}{L}\right| \cos \frac{m\pi x}{L} \cos \frac{n\pi x}{L}\, dx$$

$$= \frac{L}{\pi}\left(\psi_n - \frac{\psi_{|2\alpha - n|}}{3} - \frac{\psi_{2\alpha + n}}{3} - \frac{\psi_{|4\alpha - n|}}{15} - \frac{\psi_{4\alpha + n}}{15} - \cdots\right.$$

$$\left. + \frac{\psi_{|2q\alpha - n|}}{1 - 4q^2} + \frac{\psi_{|2q\alpha + n|}}{1 - 4q^2} - \cdots\right).$$

When $n = \alpha$, the dominant mode, only the first two terms in the sum contribute significantly to S_α. Thus

$$S_\alpha \to \frac{2}{3}\frac{L}{\pi}\psi_\alpha = \frac{2}{3}\alpha A_\alpha \sin Q_\alpha .$$

When $n \neq \alpha$, we will assume that S_n can be limited to its first term. This assumption will be justified presently, at least for the significant lower-number modes, i.e., for $n < 2\alpha$. With this assumption the system of Eqs. (20) can be written

$$\begin{aligned} \dot{A}_\alpha &= A_\alpha \omega_\alpha \sin Q_\alpha \cos Q_\alpha \left(1 - \frac{2}{3}\frac{4f\,\delta x}{\pi(\gamma - 1)^2 I_0\, \delta t} A_\alpha \left|\sin Q_\alpha\right|\right), \\ \dot{A}_n &= A_n \omega_n \sin Q_n \cos Q_n \left(1 - \frac{4f\,\delta x}{\pi(\gamma - 1)^2 I_0\, \delta t} A_\alpha \left|\sin Q_\alpha\right|\right), \qquad n \neq \alpha. \end{aligned} \tag{21}$$

Since these equations have been derived on the basis of the dominant mode assumption, which became effective at the close of Phase I of the process, they are appropriate for a description of quasi-equilibrium and equilibrium conditions, that is, Phases II and III. Without solving them we may notice their late-time properties. The rate of change of all the modes depends upon the magnitude of A_α, which will continue to increase,

on the average, as long as the bracket term in the first equation is positive. Before this growth stops, however, the bracket term in the equation for A_n, $n \neq \alpha$, will have become negative. Thus the final, Phase III, equilibrium should correspond to

$$A_\alpha \rightarrow \frac{3}{2} \frac{\pi(\gamma - 1)^2 I_0 \delta t}{4f \delta x < |\sin Q_\alpha| >} = \frac{3\pi^2(\gamma - 1)^2 I_0 \delta t}{16f \delta x}, \qquad (22)$$

$$A_n \rightarrow 0, \qquad n \neq \alpha,$$

where $< >$ signifies an average over time. However, there is some evidence to indicate that the equilibrium amplitude for A_α may be changed somewhat by the effect of the sinusoidal terms in the expression for $\dot{A}_\alpha$. This matter will be returned to again below.

Phase II is that period, following the initial amplitude growth, when the system is approaching this single frequency oscillation. Its duration varies considerably from problem to problem and is, as shall be demonstrated, largely dependent upon the number of the dominant mode. Furthermore, the number of the dominant mode increases with system size, so that ultimately the rate of energy concentration depends upon the system size. This fact is very much in evidence in the kinetic energy profiles of Fig. 2. The 6, 12, and 18 cell systems, for which Fourier decompositions indicate the lowest frequency mode is dominant, pass rapidly from initial damping to the Phase III equilibrium condition of a uniform amplitude, single frequency oscillation. But the larger systems, which are dominated by higher frequency modes, exhibit profiles indicative of composite frequency oscillations. Furthermore, the amplitude of these

kinetic energy curves increases with time, indicating a slow growth in the magnitude of the dominant mode at the expense of the secondary modes.

The variation in the calculation time required to attain a true dominant mode distribution of energy and the dependence of this calculation time upon system size are apparent from Table 1, which shows the amplitude of various modes at the completion of the machine runs. This completion time is quite arbitrary in that, although all the problems have passed the stage of initial amplitude growth, there is a marked contrast in the amount of energy concentration which has taken place. The 12 cell system is the only one in which essentially all the energy of the system has been concentrated in one mode. The other problems, one of which was run considerably longer than the 12 cell problem, all contain secondary modes of significant amplitude.

We have not been able to predict a priori which mode will dominate nor to explain why the number of the dominant mode increases with the number of cells in the system; but we can show qualitatively why the secondary mode amplitudes recede more slowly when the dominant mode wave number increases. For this purpose it seems appropriate to make use of Eqs. (21), even though the system has not yet reached a true dominant mode condition. They are considered applicable because the amplitude of the dominant mode is so much larger than the secondary mode amplitudes that condition (19) should be valid. Simplifying Eqs. (21) we write

$$\dot{A}_\alpha = A_\alpha \omega_\alpha \left(1 - \frac{2}{3} g A_\alpha\right),$$

$$\dot{A}_n = A_n \omega_n \left(1 - gA_\alpha\right),$$

where

$$g = \frac{4f\,\delta x < |\sin Q_\alpha| >}{\pi(\gamma - 1)^2 I_0\,\delta t}.$$

Solving the first equation, we obtain

$$A_\alpha = \frac{Re^{\omega_\alpha t}}{1 + \frac{2}{3} g\, Re^{\omega_\alpha t}},$$

where R is an arbitrary constant. Substituting this expression for A_α into the second equations yields a solution for A_n,

$$A_n = K_n \left[\frac{e^{\omega_\alpha t}}{\left(1 + \frac{2}{3} k\, Re^{\omega_\alpha t}\right)} 3/2\right]^{n/\alpha}, \qquad (23)$$

where K_n is another arbitrary constant.

Notice that as $t \to \infty$,

$$A_\alpha \to \frac{3}{2g},$$

$$A_n \to 0,$$

so that the final equilibrium solution is the same as before. But Eq. (23) indicates why this final solution is delayed as the value of α increases. When $\alpha = 1$, as in the 12 cell problem, the smallest possible value of the exponent is three, so that all the secondary modes lose amplitude rapidly; but for larger values of α there exist modes for which this exponent is

approximately one, so that the decay of these amplitude curves is much more gradual.

Likewise this equation demonstrates why, for a fixed value of α, the high frequency vibrations are damped much more rapidly than the lower frequency ones, substantiating our assumption that the high frequency contributions to S_n could be neglected when $n < 2\alpha$. This rapid decay of the high frequency modes is apparent in Table 2, which, for a system of 40 cells, compares the amplitude of significant modes at an earlier Phase II time with those at problem completion time as listed in Table 1. Notice also, in Table 2, the growth of the dominant mode amplitude.

TABLE 2

AMPLITUDE OF SIGNIFICANT MODES AT EARLY AND LATER EQUILIBRIUM TIMES FOR A SYSTEM OF 40 CELLS

Time	Mode Number						
	1	3	5	7	9	11	13
7,300	0.015	0.016	0.053	0.093	0.061	0.022	0.017
13,700	0.015	0.014	0.051	0.121	0.011	0.001	0.004

Now as the amplitude of these high frequency vibrations begins to change rapidly, their phase angles once again assume a strong time dependency as a result of the condition expressed in Eq. (15). These complications are made apparent in the computer results by rather erratic variations in the amplitude and period of these high frequency oscillations at late times. The irregular character of these oscillations is indicated in

Table 1 by parentheses around their average amplitude value.

On the other hand, in the larger systems, the lower frequency oscillations are extremely uniform in both amplitude and period at the time that these computer runs were completed. This would indicate that the dominant mode amplitude has not as yet changed much from the value which would make $\dot{A}_n = 0$ in Eq. (21), i.e.,

$$A_\alpha \approx \frac{\pi^2(\gamma - 1)^2 I_0 \, \delta t}{\delta f \, \delta x} \, . \tag{24}$$

And, indeed, the dominant amplitudes in Table 1 do not vary much from this value; the greatest variation is 13%.

Since this rather slow rate of growth of the dominant mode is somewhat at odds with what one would predict from Eqs. (21), it is perhaps worthy of some additional comment. Notice in these equations that the expression for $\dot{A}_\alpha$ is a product of two factors,

$$A_\alpha \, \omega_\alpha \sin Q_\alpha \cos Q_\alpha$$

and

$$\left(1 - \frac{2}{3} \frac{4f \, \delta x}{\pi(\gamma - 1)^2 I_0 \, \delta t} \, A_\alpha \left|\sin Q_\alpha\right|\right) .$$

The term in parentheses is positive for the Phase II dominant mode amplitudes given by Eq. (24), and hence any slowing down of the rate of growth must result from the first term. This could happen if the first term was approaching an oscillating function of time, in which case the product of the two terms would oscillate and A_α would experience alternating periods

of growth and decay. As this first term becomes a sinusoidal function, $\dot{A}_\alpha$ vanishes on the average and the system reaches final equilibrium.

There is some reason to believe that the final equilibrium state, which these machine problems are approaching, is characterized more by the sinusoidal nature of this first term than by the vanishing of the term in parentheses. Evidence in support of this is given by the amplitude of the dominant mode of the 12 cell system at problem completion time. Both the extreme concentration of energy into a single mode, evident in Table 1, and the uniform kinetic energy amplitude of Fig. 2b indicate that this 12 cell problem is at least very close to a final equilibrium state. And yet the dominant mode amplitude for this problem is 0.140, which is only 76% of the value that would make the term in parentheses in Eq. (21) vanish. Hence the constancy of the dominant mode amplitude must result from the vanishing on the average of the first term.

This matter will be referred to again in the discussion of final kinetic energy predictions.

Predictions

Consider, now, an estimate of the total kinetic energy of the system on the basis of this Phase II dominant mode amplitude [Eq. (24)]. The kinetic energy in the jth cell is given by

$$KE_{j-1/2} = \frac{m}{2} \sum_m \sum_n A_m \sin \frac{m\pi(j - \frac{1}{2})}{N} \sin Q_m A_n \sin \frac{n\pi(j - \frac{1}{2})}{N} \sin Q_n,$$

so that, with m = 1,

$$< KE_{j-1/2} > = \frac{1}{4} \sum_n A_n^2 \sin^2 \frac{n\pi(j - \frac{1}{2})}{N},$$

and

$$< KE > = \sum_j < KE_{j-1/2} > = \frac{N}{8} \sum_n A_n^2 \, .$$

Assuming that the dominant mode contains essentially all of the energy in the system, we have

$$< KE > = \frac{N}{8} \left[\frac{\pi^2 (\gamma - 1)^2 I_0 \, \delta t}{8f \, \delta x} \right]^2 . \qquad (25)$$

This prediction is shown as the middle line in Fig. 3. The agreement is considerably better (at this stage) than that obtained in the first analysis; most of the discrepancy can be attributed to the actual strength of the neglected secondary modes.

But from this intermediate stage of equilibrium we expect the kinetic energy profile to rise rather slowly as the dominant mode amplitude approaches its asymptotic value given by Eq. (22). Since the asymptotic dominant mode amplitude is 3/2 the value used in the kinetic energy determination above, we might expect that the kinetic energy of the system would eventually attain a level 9/4 higher than this intermediate plane. However, it is probable that this growth will be tempered by the fact that, as $\dot{A}_\alpha$ becomes small, the first factor in the expression for $\dot{A}_\alpha$ will become sinusoidal, so that $\dot{A}_\alpha$ will become an oscillating function of time in Eq. (21). The final kinetic energy level should then lie at some intermediate plateau, probably not far removed from the prediction made by the first analysis. Unfortunately, a prohibitive amount of machine time would be required to enable one of these large systems to reach this ultimate goal.

It is also possible to obtain a fairly accurate estimate of the frequency of the dominant mode at equilibrium. When the system has attained a true dominant mode energy distribution, indicative of Phase III equilibrium, and the dominant mode is approaching its limiting value, then its frequency should be approaching the natural frequency, since $\dot{\varphi}_\alpha \to 0$ with $\dot{A}_\alpha$, according to Eq. (15). In the 12 cell system, which is a case of this type, the frequency of the first mode differs by less than 2% from its natural frequency.

But for a system which has only attained the intermediate stage of equilibrium, a prediction is somewhat more difficult to obtain. The relationship between the amplitude and phase of the dominant mode in such a system is described by Eqs. (21) and (15),

$$\dot{A}_\alpha = \frac{1}{2} A_\alpha \sin 2Q_\alpha \left(\omega_\alpha - ZA_\alpha \left|\sin Q_\alpha\right|\right), \quad Z = \frac{8\alpha f \delta x}{3L(\gamma - 1)\sqrt{I_0}\,\delta t},$$

$$\dot{A}_\alpha \sin Q_\alpha + A_\alpha (\dot{Q}_\alpha - \omega_\alpha) \cos Q_\alpha = 0.$$

Since the experimental evidence indicates that the amplitude and period of the dominant mode vary quite slowly at this stage, let us set

$$A_\alpha = K + \zeta,$$

$$Q_\alpha = \Omega t + \epsilon$$

in these equations, where ζ and ϵ are higher order correction terms. Neglecting higher order terms, we get

$$\dot{\zeta} = \frac{1}{2} K \sin 2\Omega t \,(\omega_\alpha - ZK\left|\sin \Omega t\right|),$$

$$\dot{\zeta} \sin \Omega t + K(\Omega - \omega_\alpha + \dot{\epsilon}) \cos(\Omega t + \epsilon) = 0,$$

or

$$\sin 2\Omega t\,(\omega_\alpha - 2K|\sin \Omega t|) + \Omega - \omega_\alpha + \dot{\epsilon} = 0.$$

Now average over time and assume that $\langle \dot{\epsilon} \rangle = 0$ to get

$$\Omega = \frac{\omega_\alpha}{2} + \frac{4ZK}{3\pi}.$$

For K use the Phase II dominant mode amplitude given by Eq. (24). Then

$$\Omega = \frac{\omega_\alpha}{2} + \frac{4}{3\pi} \frac{8\alpha f\, \delta x}{3L(\gamma - 1)\sqrt{I_0}\, \delta t} \frac{\pi^2(\gamma - 1)^2 I_0\, \delta t}{8f\, \delta x} = \frac{17}{18}\omega_\alpha.$$

Table 3 shows a comparison of this predicted dominant mode frequency with the observed results for problems at this intermediate stage of equilibrium.

TABLE 3

COMPARISON BETWEEN OBSERVED AND PREDICTED DOMINANT MODE FREQUENCIES AT THE INTERMEDIATE STAGE OF EQUILIBRIUM

Frequency	Number of Cells			
	30	40	65	80
Observed	0.427	0.331	0.370	--
$\Omega = \frac{17}{18}\omega_\alpha$	0.439	0.329	0.375	0.323

Application to the PIC Equations

The results which have been obtained up to now have been applicable to a simplified version of the PIC equations. We should like to investigate the extent to which these results apply to the complete PIC equations.

The primary simplification made was the abandoning of the motion of particles entirely and the assumption that every cell had constant density; the resulting equations are expressed as Eqs. (1). Then, for ease of analysis, these equations were further simplified by linearizing the energy equation.

Let us consider, first, the effect of this latter modification on equilibrium attainment. Figure 4 shows the kinetic energy histories for two problems, both of which consisted of 40 cell systems with the same input data as the problems in Fig. 2. The dashed lines in the figure duplicate Fig. 2e, while the solid lines represent the maximum and minimum kinetic energy values for a problem in which the nonlinear terms in the energy equation were retained. The average late time equilibrium kinetic energy is 0.083 for the linearized version as opposed to 0.081 for the nonlinear form. The reason why the discrepancy is so slight is that each term in the nonlinear energy equation is of higher order in the perturbation than the corresponding term in the momentum equation. Because the perturbation is bounded to a very low level, the effect of these higher order terms is negligible.

But the effect of the other modification, the removal of particles, was much more pronounced. For, not only was the inherent viscosity of

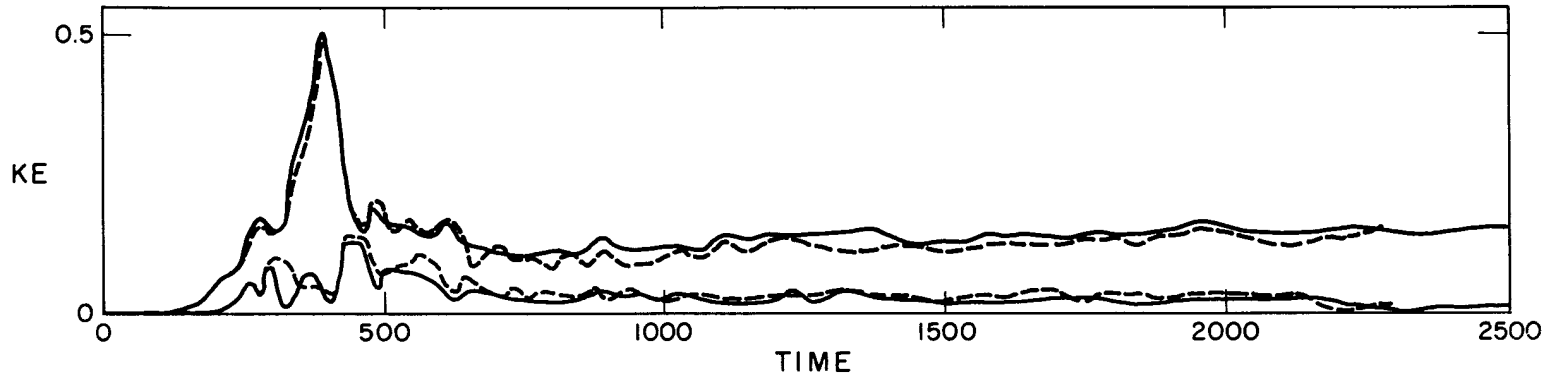

Fig. 4: A comparison between kinetic energy histories of 40 cell PIC-like systems employing linear and nonlinear versions of the energy equation. The dashed lines duplicate Fig. 2e, while the solid lines trace the maximum and minimum values of kinetic energy for a system in which nonlinear terms were retained in the energy equation.

the method, which results from particles crossing cell boundaries, lost to the system but, in addition, the system was deprived of the damping effects of momentum and energy conservation. The result is that the energy profiles of a PIC problem are bounded to a much lower level than the foregoing analysis would indicate and, furthermore, the damping effect is apparent much sooner than was the case for the simplified method. These improvements are very much in evidence in Fig. 5, which shows the kinetic energy profiles for a PIC problem of 40 cells with the same input as the problems of Fig. 4 and with 4 particles per cell.

But the presence of particles is not enough to insure effective damping of fluctuations; the number of particles per cell is also extremely important. There seems to be an optimum number of particles per cell, below which effective damping is not attained and above which only minor improvement is observed. In illustration, Table 4 lists the equilibrium kinetic energy at late times of 2, 4, and 8 particles per cell versions of the 40 cell problem illustrated in Fig. 5.

TABLE 4

EQUILIBRIUM KINETIC ENERGY AMPLITUDES OBSERVED FOR 40 CELL SYSTEMS CONSISTING OF 2, 4, and 8 PARTICLES PER CELL

Particles per Cell	Equilibrium K. E.
2	~ 0.3
4	0.020
8	0.014

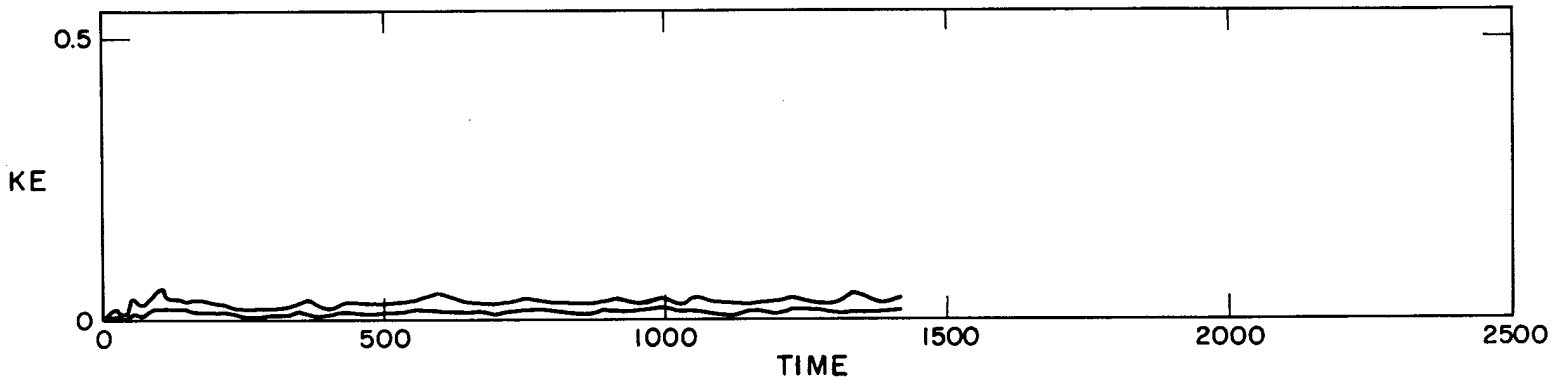

Fig. 5: Kinetic energy history for a 40 cell PIC system which has been perturbed from steady state. Each cell contains 4 particles of mass 0.25; otherwise input is the same as that of Fig. 2e.

However, it should not be thought that the requirement that a system contain a minimum number of particles per cell, on the average, constitutes a new restriction on the PIC method. It merely reflects the need for proper resolution of the fluid within the cells.

Once this basic requirement is satisfied, it appears that the relationship between equilibrium kinetic energy and the parameters f, δt, and δx, which was obtained from the analysis of the simplified equations [Eq. (25)], holds at least qualitatively for the PIC equations as well. But, whereas that analysis predicted that the equilibrium kinetic energy would vary quadratically with the ratio $\delta t/(f\ \delta x)$, the PIC experiments indicate that the variation is slower than that and depends upon the parameter which is changed in the ratio. Furthermore, in a PIC problem the permissible fluctuation of kinetic energy (and therefore the size of the ratio) is limited by the fact that velocities must remain well below the magnitude by which particles can be moved one cell length in a time cycle, i.e., $|u| < \delta x/\delta t$. Once this condition is violated, the fluctuations will no longer be bounded in amplitude.

Figure 6 shows the kinetic energy histories for a series of problems in which the ratio above is halved by varying each of the parameters in turn. The top profile is a duplicate of that in Fig. 5 except that the vertical scale is doubled in Fig. 6. The next three profiles in this figure demonstrate the effect on kinetic energy of doubling the viscosity coefficient, f, and the cell length, δx, and of halving the time interval, δt, respectively. Note that the change in the time increment had a much

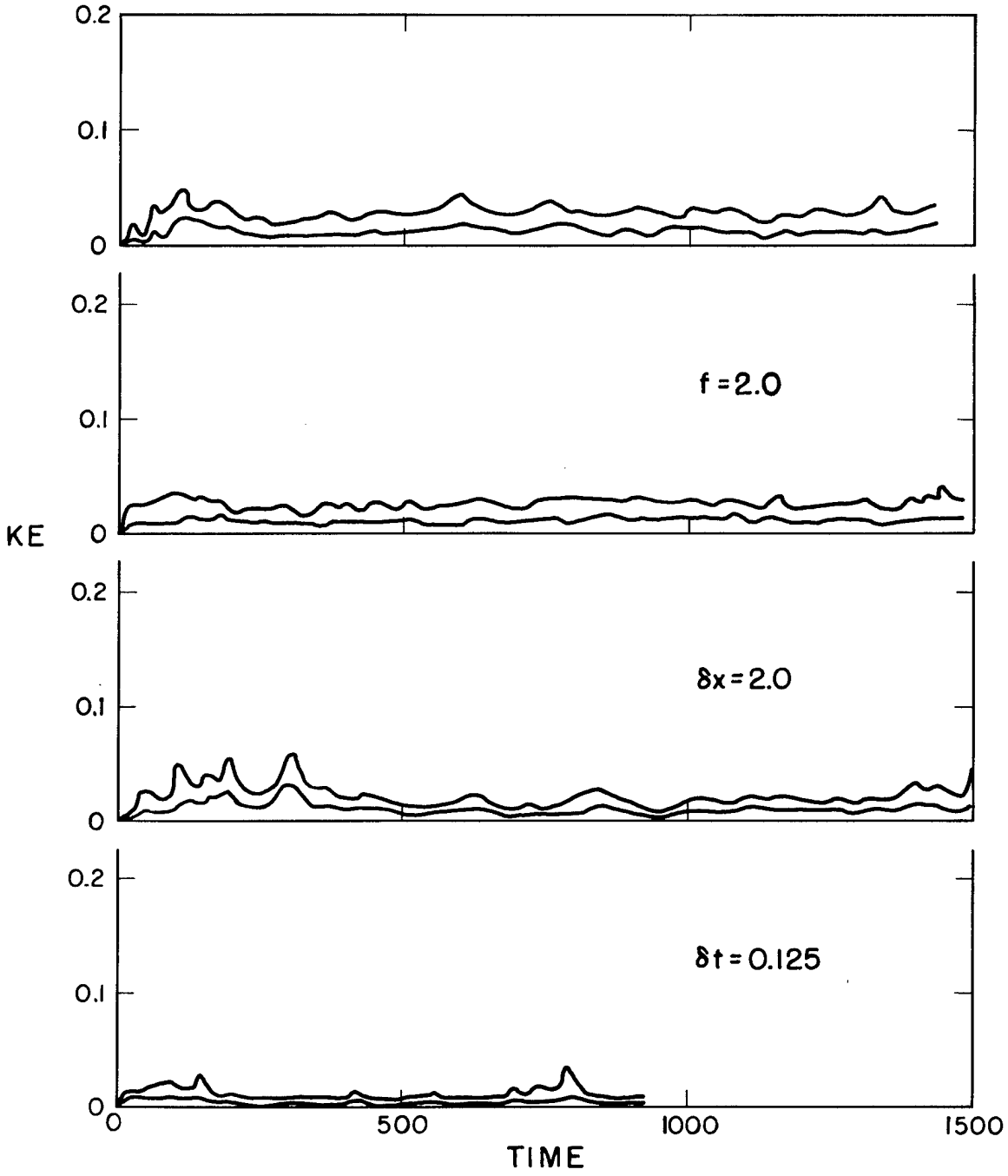

Fig. 6: This series demonstrates the effect of various parameters on the kinetic energy history of a 40 cell PIC system which has been perturbed from steady state. Except for the changes noted, the input data is the same as that for Fig. 2e, in particular, f = 1.0, δx = 1.0, δt = 0.25.

greater effect on the kinetic energy profile than either of the other parameter changes.

The importance of the time increment on instability bounding, as compared to the effect of the other parameters, persists even to zero values of the artificial viscosity. This is evident in Fig. 7 which shows the effect of doubling the cell length and halving the time interval in a system in which the only viscosity present is the effective viscosity of the PIC method (Appendix II).

A comparison of Figs. 6 and 7 is demonstrative of the fact that the introduction of nonlinear artificial viscosity into a PIC calculation will not accomplish a great deal in the way of instability bounding. This means of controlling fluctuations in what should be a stagnant region of the fluid should especially be avoided in problems where one expects large velocity gradients. A far better way of controlling these fluctuations is to place an upper limit on the time increment. Once the other parameters of the system have been chosen, this limit may be determined by introducing a perturbation into an otherwise stagnant system and varying the size of the time interval until a tolerable kinetic energy level is obtained. In many cases the limit on the time increment thus determined is less restrictive than that required to preserve stability in the regions of high velocity flow.

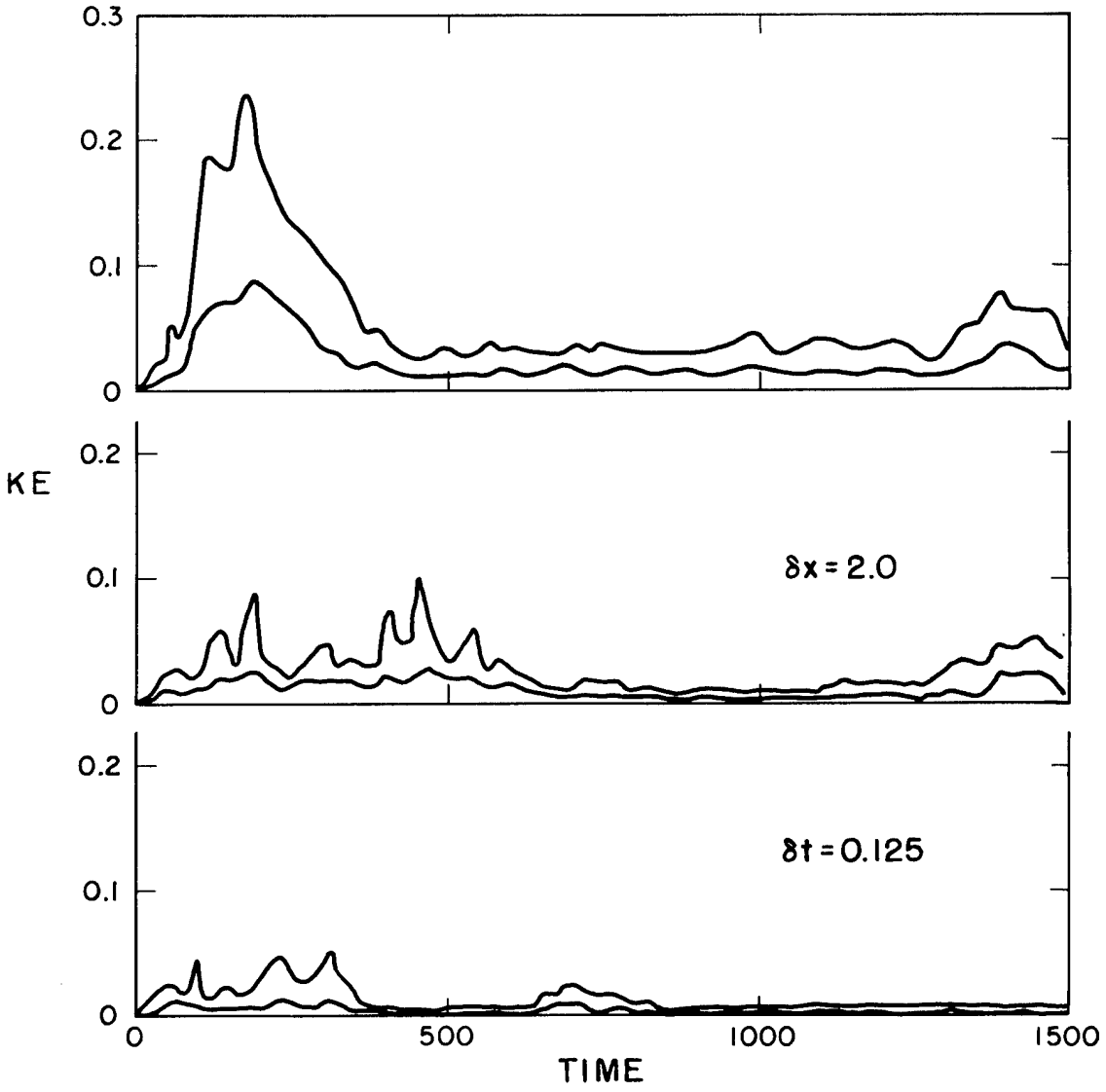

Fig. 7: Kinetic energy profiles demonstrating the effect of changes in the space and time increments of a 40 cell PIC system which is entirely free of artificial viscosity. Except for the changes noted by each profile and the fact that f = 0, the input data is the same as that of Fig. 2e.

APPENDIX I. THE FORM OF THE PIC ENERGY EQUATION

In the original PIC method the energy difference equation was derived from the differential equation

$$\rho \frac{\partial E}{\partial t} + \rho u \frac{\partial E}{\partial x} = - \frac{\partial (pu)}{\partial x}, \qquad \text{(A-1)}$$

where E is the total energy (the other quantities were defined in Part I). Using this difference scheme the method was nonconservative of energy in Phase I.

Energy conservation can be obtained in the PIC method by using as a basis for the energy difference equation the differential equation

$$\rho \frac{\partial I}{\partial t} + \rho u \frac{\partial I}{\partial x} = -p \frac{\partial u}{\partial x},$$

which is equivalent to Eq. (A-1). Dropping the transport term in this equation and transforming to difference notation we have

$$\frac{N_j m}{\delta x} \frac{\partial I_{j-1/2}}{\partial t} = \frac{p_{j-1/2}}{2\delta x} \left(u_{j-3/2} - u_{j+1/2} \right),$$

where N_j represents the number of particles in cell j and m is the mass of a particle. The velocity, u, in this equation is then replaced by its time average over Phase I, $\bar{u}$. With this change the Phase I momentum and

energy equations, with artificial viscosity terms neglected, appear as follows:

$$\tilde{u}_{j-1/2} = u^n_{j-1/2} + \frac{\delta t}{2N^n_j m}\left(p^n_{j-3/2} - p^n_{j+1/2}\right), \tag{A-2}$$

$$\tilde{I}_{j-1/2} = I^n_{j-1/2} + \frac{\delta t\, p^n_{j-1/2}}{2N^n_j m}\left(\bar{u}_{j-3/2} - \bar{u}_{j+1/2}\right),$$

where the tilde symbolizes the fact that these terms do not as yet include the transport effect.

To see that this differencing technique, together with the proper boundary conditions, does conserve total energy, observe that at time t the total energy of the system is

$$E^n = \sum_{j=1}^{J} N^n_j m\left[I^n_{j-1/2} + \frac{1}{2}\left(u^n_{j-1/2}\right)^2\right],$$

whereas by the end of Phase I it has changed to

$$\tilde{E} = \sum_{j=1}^{J} N^n_j m\left[\tilde{I}_{j-1/2} + \frac{1}{2}\left(\tilde{u}_{j-1/2}\right)^2\right],$$

the total change being

$$\delta E = \sum_{j=1}^{J} N^n_j m\left[\tilde{I}_{j-1/2} - I^n_{j-1/2} + \bar{u}_{j-1/2}\left(\tilde{u}_{j-1/2} - u^n_{j-1/2}\right)\right],$$

$$\delta E = \frac{\delta t}{2}\sum_{j=1}^{J}\left[\left(p^n_{j-1/2}\bar{u}_{j-3/2} + p^n_{j-3/2}\bar{u}_{j-1/2}\right)\right. \tag{A-3}$$

$$\left. - \left(p^n_{j+1/2}\bar{u}_{j-1/2} + p^n_{j-1/2}\bar{u}_{j+1/2}\right)\right],$$

after rearrangement of terms. This equation is now in conservative form and, in terms of the fictitious cells beyond the system ($j = 0$ and $j = J + 1$), can be written

$$\delta E = \frac{\delta t}{2}\left(p^n_{1/2}\bar{u}_{-1/2} + p^n_{-1/2}\bar{u}_{1/2} - p^n_{J+1/2}\bar{u}_{J-1/2} - p^n_{J-1/2}\bar{u}_{J+1/2}\right).$$

Since the system is considered to have rigid boundaries the velocity must vanish at both ends; thus $u_{-1/2} = -u_{1/2}$ and $u_{J-1/2} = -u_{J+1/2}$ always. Likewise $du/dt = 0$ at each boundary so that $p_{-1/2} = p_{1/2}$ and $p_{J-1/2} = p_{J+1/2}$ by Eq. (A-2). Energy conservation then follows from these boundary conditions.

APPENDIX II. ARTIFICIAL VISCOSITY

Inherent in the PIC method is a diffusion term which is proportional to velocity magnitude. This was demonstrated in Reference 1, p. 15 ff, by forming the Taylor expansions of the difference equations which represent all three phases of the PIC method. The resulting equations, with higher order terms neglected and subscripts dropped, were

$$\rho \frac{\partial u}{\partial t} + \rho u \frac{\partial u}{\partial x} = - \frac{\partial p}{\partial x} + \frac{\partial}{\partial x}\left(\lambda' \frac{\partial u}{\partial x}\right),$$

$$\rho \frac{\partial I}{\partial t} + \rho u \frac{\partial I}{\partial x} = - p \frac{\partial u}{\partial x} + \frac{\partial}{\partial x}\left(\lambda' \frac{\partial I}{\partial x}\right) + \lambda' \left(\frac{\partial u}{\partial x}\right)^2,$$

where

$$\lambda' = \frac{1}{2} \delta x \, \rho u$$

is called the effective viscosity coefficient. Comparing these equations with the momentum and energy equations expressing one dimensional compressible fluid flow,

$$\rho \frac{\partial u}{\partial t} + \rho u \frac{\partial u}{\partial x} = - \frac{\partial p}{\partial x},$$

$$\rho \frac{\partial I}{\partial t} + \rho u \frac{\partial I}{\partial x} = - p \frac{\partial u}{\partial x}$$

demonstrates that the λ' terms have their origin in the difference method.

The λ' terms have their principal effectiveness in regions where the velocity gradient is large or where fluctuations occur in high speed material. In fact, it is due to the presence of these terms that the PIC method achieves success in approximating high velocity fluid flow. This measure of success has not been obtained in problems in which the fluid speed is considerably subsonic.

Specifically, an important limitation of the PIC method exists when perturbations are introduced into an otherwise stagnant fluid. Large fluctuations about the proper values develop in the region of the perturbation. Damping of these fluctuations will only develop as the velocity increases to the point where the effective viscosity becomes important. In order to obtain rapid damping in a nearly stagnant fluid, a dissipative force not proportional to velocity is required.

Provision has been made in the PIC method to introduce, artifically, variable amounts of damping forces in the form of pressure modifications. This dissipative term is of the form

$$q_j^n = \rho_j^n \left(ac_0 + \frac{f}{2} \left| u_{j-1/2}^n + u_{j+1/2}^n \right| \right) \left(u_{j-1/2}^n - u_{j+1/2}^n \right)$$

and is always calculated at cell boundaries.

The ac_0 part of q is of the type discussed above since it is not proportional to velocity. It is similar to a Landshoff [4] artificial viscosity in that c_0 is taken as a representative sound speed for the system. This portion of the dissipative force is applied only when the system is experiencing compression.

In Part I it was demonstrated (p. 15) that the PIC equations were unconditionally unstable for

$$ac_0 < \left(1 + \cos\frac{\pi}{N}\right)\frac{(\gamma - 1)^2\ \delta t\ I_0}{2\delta x}.$$

This instability is bounded in amplitude, however, by the effective viscosity of the PIC method. A comparison of the recovery from a density perturbation away from steady state is shown in Fig. A-1 for systems which contain ac_0 type viscosity, f type viscosity, and effective viscosity only. Notice that recovery is complete in the presence of ac_0 type viscosity but that a finite equilibrium amplitude is approached in the other two cases (see Part II).

The f part of the artificial viscosity is proportional to the effective viscosity. It may be applied either in compressions and rarefactions or in rarefactions alone. Thus one is permitted a rather wide choice in either bolstering, reducing, or removing the effective viscosity of the system. Such a capability is important in those problems in which effective viscosity has a detrimental effect. As an example, when gas moves away from a wall the effective viscosity can cause cavitation by smoothing the velocity profile. In this case removing effective viscosity only in rarefactions prevents cavitation while retaining the smoothing effect in compressions.

However, in most problems in which a rather wide range of velocity values is encountered, better smoothing seems to be obtainable from the ac_0 type of viscosity than from any other type. As an example, when a

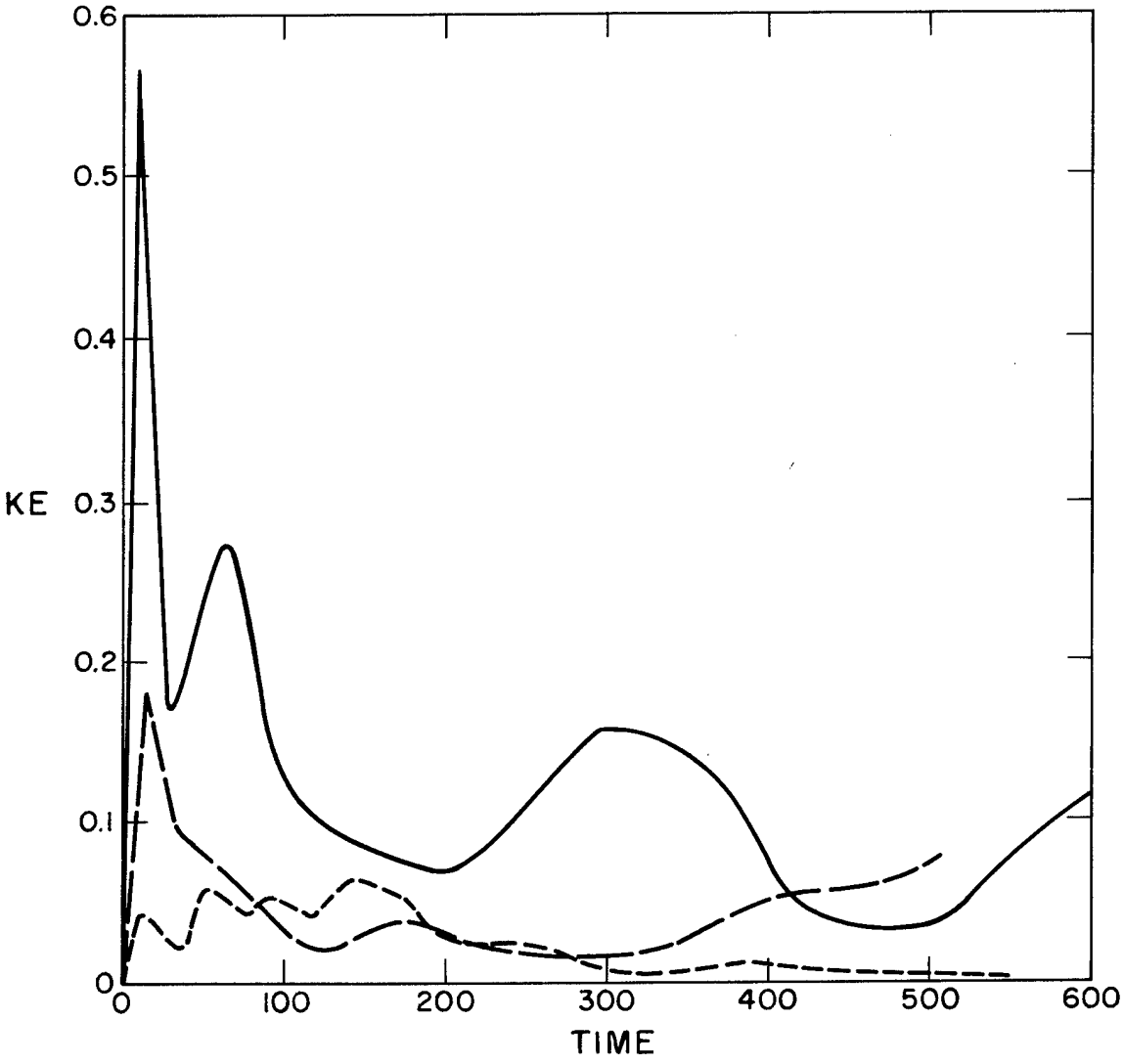

Fig. A-1: Profiles of maximum kinetic energy from three 20 cell PIC systems which have been perturbed from steady state as the result of an instantaneous density imbalance. The dotted line profile resulted from calculations employing linear artificial viscosity ($ac_0 = 1.0$), the dashed line profile corresponds to nonlinear artificial viscosity ($f = 1.0$), and the solid line to a system which did not employ artificial viscosity.

plane steady shock strikes and reflects from a rigid wall, one would expect the material velocity in the vicinity of the wall to come to zero. Figure A-2 illustrates the effect on such a system of various types of viscosity. The first profile is that for a system in which the effective viscosity has been removed by setting f = -0.5, in the second case no artificial viscosity has been applied, while in the third, fourth and fifth profiles an f type, a Richtmyer-Von Neumann type, and an ac_0 type viscosity have been applied respectively, all with the viscosity coefficient set equal to 1. Notice that the best damping is obtained with the ac_0 type viscosity.

The effectiveness of the artificial viscosity terms depends to a large extent on the manner in which they are expressed in the difference equations. This is true not only in the PIC method but also in other differencing schemes.

Let us examine the effectiveness of Eqs. (A-2) when they are modified to include artificial viscosity. The obvious way to achieve this modification, without destroying the conservativeness of the system, is to replace cell pressures in those equations by the sum of the equation of state pressure for the cell plus the average value of artificial viscosity at the cell's two boundaries. But, by reason of this definition, the momentum equation becomes

$$\frac{\partial u_{j-1/2}}{\partial t} = \frac{1}{2N^n_j m}\left[\left(p^n_{j-3/2} - p^n_{j+1/2}\right) + \frac{1}{2}\left(q^n_{j-2} + q^n_{j-1} - q^n_j - q^n_{j+1}\right)\right]. \tag{A-4}$$

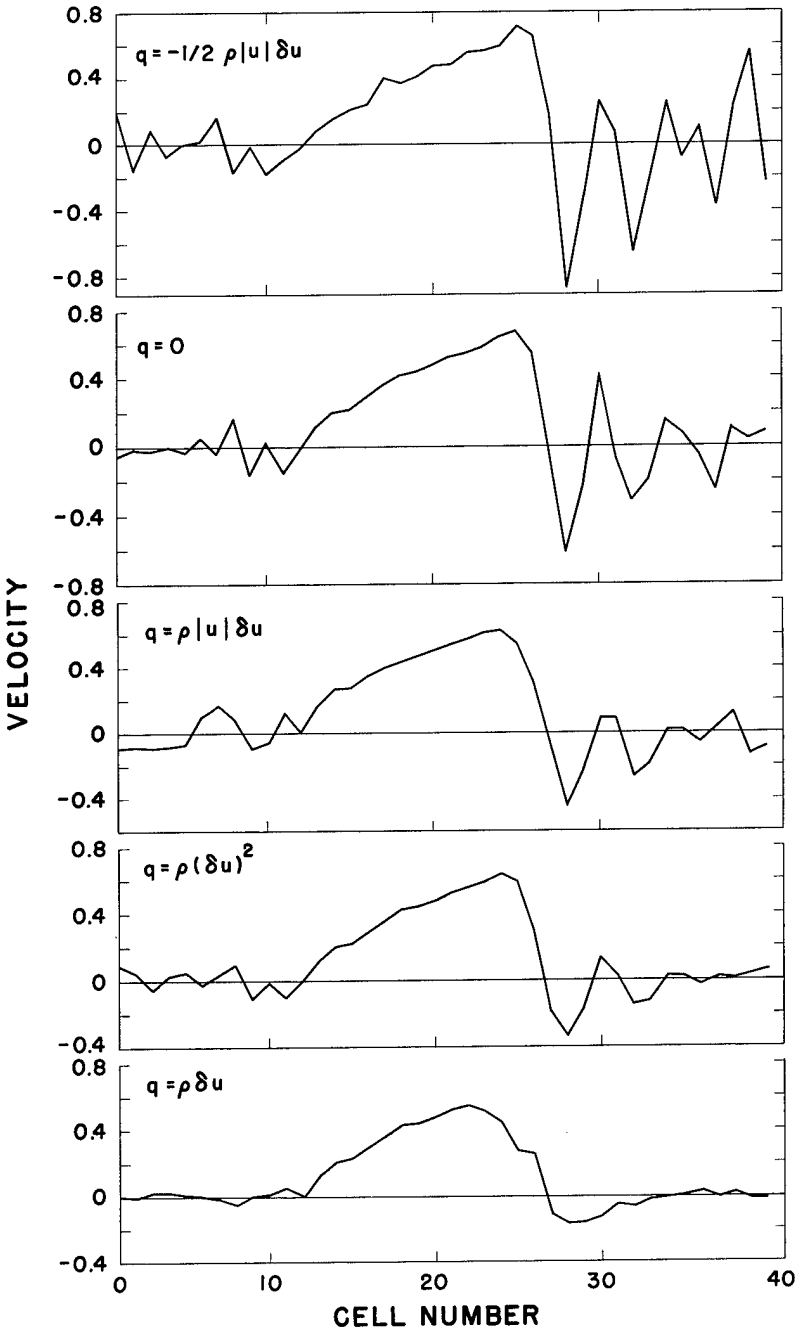

Fig. A-2: Velocity profiles of 40 cell PIC systems which show the effect of a plane steady shock striking and reflecting from a rigid wall. Each profile is labeled with the type of artificial viscosity used in its calculation.

The defect in this manner of differencing is apparent. In averaging the dissipative terms over such a wide spatial range, the sensitivity of velocity change to velocity gradient is impaired. This results in too much smoothing in the neighborhood of shocks and, at the other extreme, too little damping when perturbations occur in an otherwise stagnant fluid.

Nor can this sensitivity be achieved simply by writing the momentum equation as

$$\frac{\partial u_{j-1/2}}{\partial t} = \frac{1}{N_j^n m} \left[\frac{1}{2}\left(p^n_{j-3/2} - p^n_{j+1/2}\right) + \left(q_{j-1} - q_j\right)\right], \qquad \text{(A-5)}$$

for this destroys the energy conservation of the equations.

But it is possible to achieve difference equations which are conservative and yet do not involve interpolated viscosity terms. To do this it is necessary to alter the derivation of the Phase I equations. Begin with the one dimensional momentum and energy differential equations with transport terms dropped and pressures modified to include artificial viscosity,

$$\rho \frac{\partial u}{\partial t} = -\frac{\partial}{\partial x}(p + q),$$

$$\rho \frac{\partial I}{\partial t} = -(p + q) \frac{\partial u}{\partial x}.$$

But now rewrite the energy equation in the equivalent form

$$\rho \frac{\partial I}{\partial t} = -p \frac{\partial u}{\partial x} - \frac{\partial (qu)}{\partial x} + u \frac{\partial q}{\partial x}.$$

Using this alternate form of the energy equation, we write the equations in the difference form

$$\frac{N_j^{n\,m}}{\delta t}\left(\tilde{u}_{j-1/2} - u^n_{j-1/2}\right) = p^n_{j-1} - p^n_j + q^n_{j-1} - q^n_j$$

$$\frac{N_j^{n\,m}}{\delta t}\left(\tilde{I}_{j-1/2} - I^n_{j-1/2}\right) = p^n_{j-1/2}\left(\bar{u}_{j-1} - \bar{u}_j\right) + \left(q^n\,\bar{u}\right)_{j-1} \qquad \text{(A-6)}$$

$$- \left(q^n\,\bar{u}\right)_j + \bar{u}_{j-1/2}\left(q^n_j - q^n_{j-1}\right),$$

where we have now written the momentum equation in the form of Eq. (A-5). With the difference equations thus expressed, energy conservation is no longer a problem. For the variation in total energy over Phase I is

$$\tilde{E} - E^n = \sum_{j=1}^{J} N_j^{n\,m}\left[\tilde{I}_{j-1/2} - I^n_{j-1/2} + \bar{u}_{j-1/2}\left(\tilde{u}_{j-1/2} - u^n_{j-1/2}\right)\right]$$

$$= \delta t \sum_{j=1}^{J}\left[p^n_{j-1/2}\left(\bar{u}_{j-1} - \bar{u}_j\right) + \bar{u}_{j-1/2}\left(p^n_{j-1} - p^n_j\right)\right.$$

$$\left. + \bar{u}_{j-1/2}\left(q^n_{j-1} - q^n_j\right) - \bar{u}_{j-1/2}\left(q^n_{j-1} - q^n_j\right) + \left(q^n\,\bar{u}\right)_{j-1} - \left(q^n\,\bar{u}\right)_j\right],$$

which is clearly in conservative form.

All of the problems described in this report made use of the computing scheme described by Eqs. (A-6).

REFERENCES

1. Evans, M. W., and Harlow, F. H., "The Particle-in-Cell Method for Hydrodynamic Calculations," Los Alamos Scientific Laboratory Report LA-2139, June, 1957.

2. Harlow, F. H., et al., "Two-Dimensional Hydrodynamic Calculations," Los Alamos Scientific Laboratory Report LA-2301, April, 1959.

3. Kryloff, N., and Bogoliuboff, N., "Introduction to Nonlinear Mechanics," Annals of Mathematical Studies, Number 11, Princeton University Press, 1947.

4. Landshoff, R., "A Numerical Method for Treating Fluid Flow in the Presence of Shocks," Los Alamos Scientific Laboratory Report LA-1930, 1955.